Journal of Materials Chemistry

Cite this: J. Mater. Chem., 2012, 22, 8662

www.rsc.org/materials

PAPER

Bone regeneration: importance of local pH—strontium-doped borosilicate scaffold

Yuhui Shen,†[a] Waiching Liu,†[b] Chunyi Wen,[b] Haobo Pan,*[bc] Ting Wang,[b] Brian W Darvell,[d] William W Lu[bc] and Wenhai Huang[e]

Received 24th November 2011, Accepted 24th February 2012
DOI: 10.1039/c2jm16141a

The effect of local pH on bone regeneration has never been properly studied or discussed. However, using a microelectrode, the pH on the surface of implant materials, rather than in the bulk, is measurable so that the biological response based on the local environment can be studied. It was found that the osteoblast viability was significantly enhanced with an increase of pH, to an optimum level at ~pH 8–8.5; in contrast, the activity fell markedly below pH 6. The effect of strontium on osteoblast proliferation was further increased at pH ~8, suggesting a possible new approach for enhancing its activity in the treatment of osteoporosis. No stimulation of osteoblast proliferation was found for boron at normal physiological pH but, surprisingly, such an effect was found at pH 8.5. For the degradation of strontium-doped borosilicate, the ambient alkaline pH not only enhanced the activity of strontium and boron, but also facilitated the nucleation of apatite, as indicated by the newly formed bony tissue. Consequently, appropriately designed biomaterials, which create such an ideal ambient alkaline environment for bone regeneration, may be crucial aspects for bone substitutes.

1. Introduction

Bone is formed by the mineralization of an organic matrix (largely collagen), with the nucleation and growth of a mineral closely similar to hydroxyapatite (HA), through a complex cascade of events involving the proliferation of primitive mesenchymal stem cells, differentiation into osteoblastic precursor cells (osteoprogenitor cells and preosteoblasts), maturation of osteoblasts, formation of a matrix and ultimately mineralization.[1] The activity of the osteoblasts is regulated by various hormones and local factors such as oestrogen, parathyroid hormone (PTH) and bone morphogenetic proteins. The expression of these factors results in the occurrence of demineralization and remineralization in a dynamic balance. Critically, this process must depend on whether osteoblasts are influenced for good or ill by solutes arising from any implant. The uncertainty lies in the fact that the local microenvironment can be affected by the resorption of the implant through, for example, ion concentrations, depending on the specifics of the interaction between the adjacent tissue and the material implanted. In turn, the local pH around the implant may be shifted from the physiologically-normal value.

Current pharmaceutical therapies, including the systemic administration of PTH,[2] anti-sclerostin antibodies,[3] calcium with vitamin D,[4] and alendronate,[5] have been shown to maintain bone mineral density, alleviate bone loss and thus decrease the risks of bone fracture. Although these treatments focus on modulating the activities of either osteoblasts or osteoclasts, or both, little attention has been paid to the milieu wherein the cells reside, and in particular to its pH. One long-standing observation is that extracellular pH regulates the balance of bone resorption and formation: chronic systemic acidosis promotes resorption, whereas alkalosis promotes formation (mineralization).[6–9] Kaunitz and Yamaguchi[10] postulated that a rather high pH ~9 might exist in the microenvironment for bone formation since pH 8.5 was shown to be optimum for alkaline phosphatase (ALP) activity towards inorganic pyrophosphate, while only around 60% of the activity was retained at the 'physiological' pH ~7.4.[11] For example, it was shown that both the proliferation and ALP activity of osteoblasts were significantly enhanced with the degradation of calcium silicate, in which the pH increased to above 8 after 24 h. In contrast, a relatively lower activity was found when the pH was adjusted to 7.4.[12] In other words, the pro-mineralization activity of osteoblasts is increased at higher extracellular pH values. Consequently, appropriately designed biomaterials for bone regeneration, which create such an

[a]*Department of Orthopaedics, Shanghai Institute of Orthopaedics & Traumatology, Shanghai Ruijin Hospital, Shanghai Jiaotong University School of Medicine, China*
[b]*Department of Orthopaedics & Traumatology, The University of Hong Kong, R9-12, Lab Block, 21 Sassoon Rd., Pokfulam, Hong Kong, China. E-mail: haobo@hku.hk; Fax: (+852) 28185210; Tel: (+852) 64180653*
[c]*Center for Human Tissues and Organs Degeneration, Shenzhen Institute of Advanced Technology, Chinese Academy of Science, Shenzhen, China*
[d]*Dental Materials Science, Department of Bioclinical Sciences, Faculty of Dentistry, Kuwait*
[e]*Department of Materials Science & Engineering, TongJi University, China*
† Yuhui Shen and Waiching Liu contributed equally as the first author to the article

ambient alkaline environment higher than pH 7.4, may be critical for success.

Bioactive borosilicate glass,[13,14] a novel biodegradable material, is showing potential in bone tissue engineering. The extraordinary performance appears to be due to the controlled release of boron, which is particularly needed or beneficial for many life processes including embryogenesis, bone growth and maintenance, immune function and psychomotor skills.[15–18] Boron deficiency has been found to have a remarkable effect on the amount of calcium excretion in the urine.[19] Furthermore, for post-menopausal women, strontium-doped borosilicate glass seems to play a special role in bone remodeling as it is associated with both the stimulation of bone formation and the reduction of bone resorption.[20]

The spontaneous precipitation of HA-like minerals has been attributed to the rapid release of alkalizing ions from a glass network, thought to result in an increase of the adjacent pH,[20] since the ion activity product (IP) for such a solution with respect to $[Ca^{2+}]$, $[PO_4^{3-}]$ and $[OH^-]$ is then greater than under normal physiological conditions. Such a phenomenon is consistent with the resorption of typical 45S5 bioglass[21] and calcium silicate,[22] in both of which there is spontaneous bonding with bony tissue *via* an intermediary calcium phosphate layer. However, there appears to be no reports of the effect of pH on this process, even though the activity of osteoblasts is known to be pH-sensitive.[23,24] Unfortunately, the optimum pH for bone formation is unknown, and so the question of whether the efficiency of therapeutic strontium and boron is associated with their effect on the local pH remains open. Thus, the aim of the present work was to test and clarify this situation through an *in vitro* and *in vivo* study of plain (BSi) and strontium-doped (SrBSi) borosilicate glass scaffolds, and the role of the local pH.

2. Materials and methods

2.1 MC3T3-E1 viability

2.1.1 Cell culture. A preosteoblastic cell line (MC3T3-E1; ATCC, Manassas, VA, USA) was seeded in 96-well plates at a density of 1.2×10^4 cells/well in a modified minimum essential medium (α-MEM; GIBCO, Invitrogen, Grand Island, NY, USA) containing 10% (v/v) fetal bovine serum (Biowest, Nuaillé, Maine et Loire, France) and cultured at 37 °C under 5% CO_2 and 95% air at 100% relative humidity (RH).

2.1.2 pH effect. To study the effect of pH on cell viability, the culture medium was firstly adjusted using HCl (0.1 mmol L^{-1}) and NaOH (0.1 mmol L^{-1}) to pH values from 5.0 to 10.0 (at 0.5 intervals), while the original medium at pH 7.4 served as control. Cell viability was evaluated using the 3-(4,5-dimethylthiazol-2-yl)-2,5-diphenyl tetrazolium bromide (MTT) assay, respectively on days 1, 3 and 5. For day 5, the culture medium was replaced at day 3 with 100 μL of fresh medium at the appropriate pH. At each test time, the medium was replaced with 100 μL of fresh medium and 10 μL of 5 mg mL^{-1} MTT (Dojindo, Kumamoto, Japan) solution. After a further 4 h incubation, the medium–MTT solution was removed and replaced with 100 μL of dimethylsulfoxide (DMSO) (Wako, Osaka, Japan). After 10 min of slow shaking (Vibramax 100, Metrohm, Tampa, FL, USA), the absorbance was read at 570 nm against a reference value at 630 nm, and the result was expressed as the optical density (OD).

2.2 Effect of strontium, boron and silicon

2.2.1 Concentration. The culture medium was modified by the addition of $SrCl_2$, H_3BO_4 or Na_2SiO_3 (analytical grade, BDH, Poole, England) to concentrations of 0.1, 1.0, 2.0, 5.0 and 10.0 mmol L^{-1}, separately, all at pH 7.4. Processing was as above, with the MTT absorbance being read on days 1, 3 and 5 respectively.

2.2.2 Effect of pH on strontium, boron and silicon effects. Based on the results of the above trials, the concentrations causing the maximum OD values ([Sr] = 5 mmol L^{-1}; [B] = 1 mmol L^{-1}; [Si] = 1 mmol L^{-1}) were used to test further the effect of pH on cell viability by adjusting the above pH to values of 7.0, 8.0, 8.5 and 9.0, where the unadjusted solution (at pH 7.4) and blanks for each pH (no additive) served as separate controls. The MTT assay was again performed on days 1, 3 and 5, respectively.

2.3 Scaffold

2.3.1 Fabrication. Borosilicate glass (BSi), with a composition $6Na_2O$-$8K_2O$-8MgO-22CaO-$36B_2O_3$-$18SiO_2$-$2P_2O_5$ (*i.e.*, as molar percentages) was prepared in the conventional manner by melting appropriate reagent-grade materials (BDH, Poole, UK) in a platinum crucible at 1200 °C for 2 h with stirring, then quenching between cold stainless-steel plates. The Sr-doped borosilicate (SrBSi) was made by replacing Mg partially to give 6 mol% Sr. The quenched material was crushed and ground, and sieved to a particle size of ~4 μm.

Scaffolds of BSi and SrBSi with interconnected high porosity were fabricated using a polymer-foam replication method.[24] In essence, this involved the preparation of green bodies of glass networks by coating the internal surfaces of a polyurethane foam with a slurry of glass particles. The slurry was prepared by vigorously stirring a mixture of 3 g glass powder, 20 mL absolute ethanol (BDH) and 0.3 g ethyl cellulose (BDH). The polyurethane foam (Shanghai No. 6 Plastic Product Co. Ltd., Shanghai, China) was chosen for its similarity to the morphology of human trabecular bone, having the desired pore structure and about 2 open pores per mm. The polymer template was first filled with slurry by squeezing whilst immersed, drained and squeezed gently to remove excess, then dried in air at ambient temperature for 24 h before being heated at 2 °C min^{-1} to 450 °C for 1 h. When the polymer had been removed, the remaining glass skeleton was sintered in air at 600 °C for 1 h to obtain the desired scaffold without crystallization.

2.3.2 Characterization. The constitution and composition of the scaffold materials (BSi and SrBSi) were characterized by X-ray diffraction (XRD; Model D/max 2550V, Rigaku, Tokyo, Japan) using Cu-Kα radiation ($\lambda = 1.5406$ Å) in step-scan mode ($2\theta = 0.02°$ per step) and Fourier-transform infrared spectroscopy (FTIR; Lambda 2S, Perkin-Elmer, Waltham, MA, USA). The chemical composition was determined by inductively-coupled plasma optical-emission spectrometry (ICP-OES; 710-ES, Varian, Palo Alto, CA, USA). The failure stress in compression of

cylindrical specimens ($n = 5$; with a diameter of 6 mm and 12 mm in length) was measured using a universal testing machine (Model 4204, Instron, High Wycombe, UK) at a crosshead speed of 0.5 mm min^{-1}. The 3-D structure and the porosity were analysed using X-ray microtomography (microCT-40, Scanco Medical, Brüttisellen, Switzerland) with an isotropic voxel size of 9 μm at 100 kV. Standardized reconstruction used a modified Feldkamp algorithm in the software (NRecon, v. 1.6.4; SkyScan, Kontich, Belgium), and the data sets were characterized using proprietary software (CTAn, v. 1.10; SkyScan).

2.3.3 Degradation behaviour. Culture medium extracts were first prepared by immersing pairs of discs (~0.05 g) of the scaffold materials (3 mm diameter, 2 mm thick) to 0.1 g mL^{-1} in culture medium (*i.e.* ~2 mL) at 37 °C with incubation under 5% CO_2 and 95% air at 100% RH for 1, 2, 4, 8, 12, 24, 48 and 72 h. During the course of this, the surface and bulk solution pH were measured using a flat membrane microelectrode (MI-406, Microelectrodes, Bedford, NH, USA) with a separate reference electrode (MI-401, Microelectrodes). The surface value was obtained by gently touching the tip of the pH electrode to the material, while the reference electrode was held stationary alongside, taking care to minimize the disturbance of the medium. In a separate run, the pH of the bulk solution was measured following the removal of the test material and then stirring.[12] The elemental concentration of the extracts for Sr, B and Si was determined by ICP-OES. The surface morphology before and after 72 h immersion was observed by scanning electron microscopy (SEM; LEO 1530, Oxford, UK).

2.3.4 Cell response to extracts. To clarify the effect of pH, 24 h extracts (as above, section 2.3.3) were adjusted to pH 7.4 using HCl. The cell viability was then determined at the extract pH and after adjustment to pH 7.4 by MTT assay, as above (section 2.1.2). In addition, the alkaline phosphatase (ALP) activity was determined after 72 h culture using a colorimetric assay (Alkaline Phosphatase LiquiColor, Stanbio, Boerne, TX, USA) based on the hydrolysis of 4-nitrophenyl phosphate to 4-nitrophenol, which is formed at a rate directly proportional to the ALP activity. The absorbance was determined at 405 nm using a microplate reader (DTX 800 Multimode Detector, Beckman Coulter, Brea, CA, USA), with the data normalized by the total cell protein, as measured with a commercial kit (DC Protein Assay Kit, Bio-Rad, Hercules, CA, USA), and was expressed as micromoles of 4-nitrophenol produced per hour per milligram of protein (μmol h^{-1} mg^{-1}).

2.4 Animal studies

2.4.1 Model. All procedures involving animals met the standards set out in the guide for the care and use of laboratory animals, and were approved, by the Committee on the use of Live Animals in Teaching and Research of The University of Hong Kong (CULATR No. 2716-10). Female Sprague–Dawley rats (250 g, $n = 5$ for BSi and SrBSi groups) were operated on under general anaesthesia with 10% ketamine/2% xylazine (Kethalar, 1 mL : 1 mL); sedation was maintained with 2.5% sodium phenobarbital injected intravenously (Sigma-Aldrich, St Louis, MO, USA). With routine shaving and aseptic procedures, an incision was made to expose the medial side of the tibial shaft and a bone defect was created by drilling a 3-mm diameter hole through the shaft 5 mm below the tibial plateau. After the surgical implantation of a disk of the scaffold material (3 mm diameter, 2 mm thick), the wound was closed and dressed. The rats were allowed to move freely in the cage after surgery, and sacrificed at 4 weeks to study the new bone formation at an early stage.

2.4.2 Histology. After euthanasia, the recovered tibiae with implants were dehydrated sequentially in ethanol and xylene and then infiltrated by immersion for 7 days in 15 mL portions of a mixture of 1 L methyl methacrylate (MMA), 250 mL dibutyl phthalate and 40 g dibenzoyl peroxide, followed by curing at 37 °C overnight (~16 h). The resulting PMMA-embedded specimens were then sectioned transversely using a saw microtome (SP 1600, Leica, Germany). Sections from the middle portion of the bone tunnel were ground and polished to 40–50 μm (RotoPol-21, Struers, Denmark) and stained with Giemsa-Eosin for optical microscopy (Q500MC, Leica Cambridge, Cambridge, UK). Bone in-growth was evaluated within the defect boundaries using image analysis (Image Pro Plus 5.0 Media Cybernetics, MD, USA). The bone area, A_B, referring to the area of trabecular bone, including both mineralized bone and osteoid, in the total tissue area analysed, A_T, was found based on standardized nomenclature and definitions.[25] The bone volume fraction, V_B, expressed as a percentage was then calculated as A_B/A_T, using the stereometric equivalence.

2.4.3 Chemical analysis. The composition and constitution of the newly-formed bone in the regions corresponding to those investigated histologically were characterized by energy-dispersive X-ray analysis (EDX; LEO 1530) and XRD, respectively.

2.5 Statistical analysis

All data are expressed as mean ± standard deviation (SD), $n = 5$, and were subject to one- and two-way analysis of variance (AoV) and Tukey's multiple-comparison test. The critical value was set at $\alpha = 0.05$.

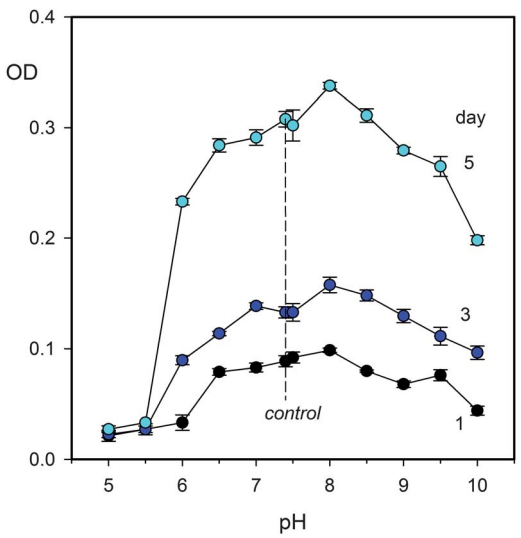

Fig. 1 Effect of pH on the MC3T3-E1 osteoblast activity.

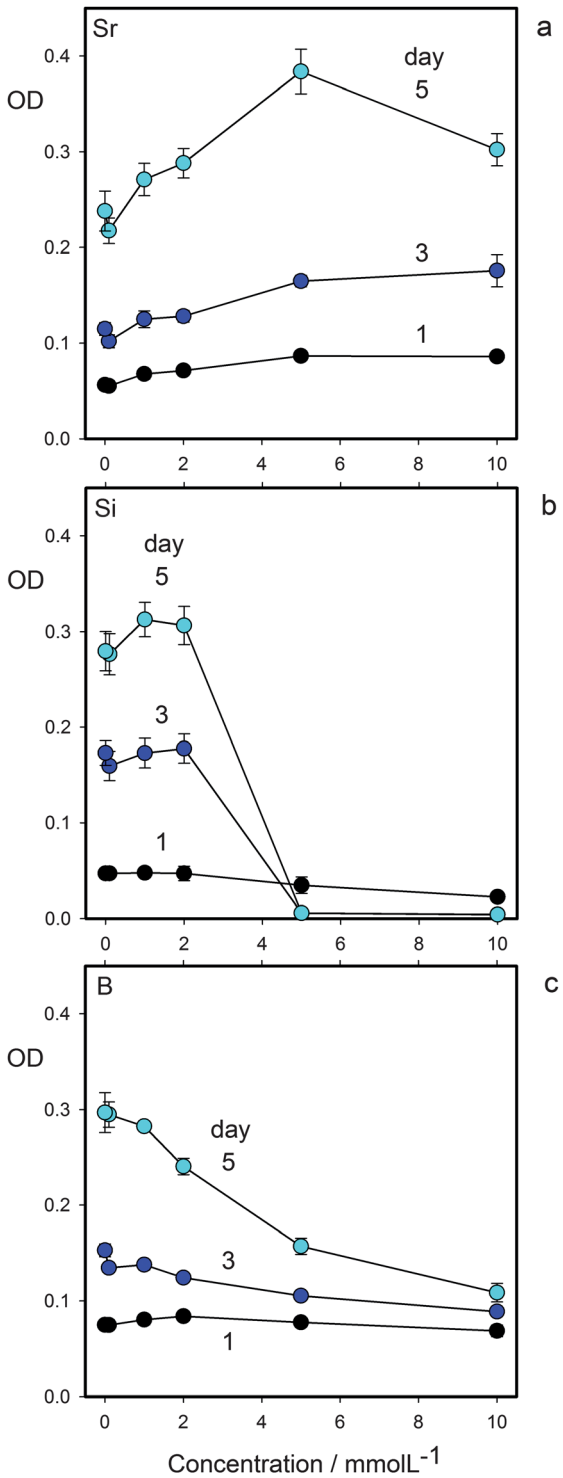

Fig. 2 Effect of the concentration of solution Sr, Si and B concentration on the MC3T3-E1 osteoblast activity.

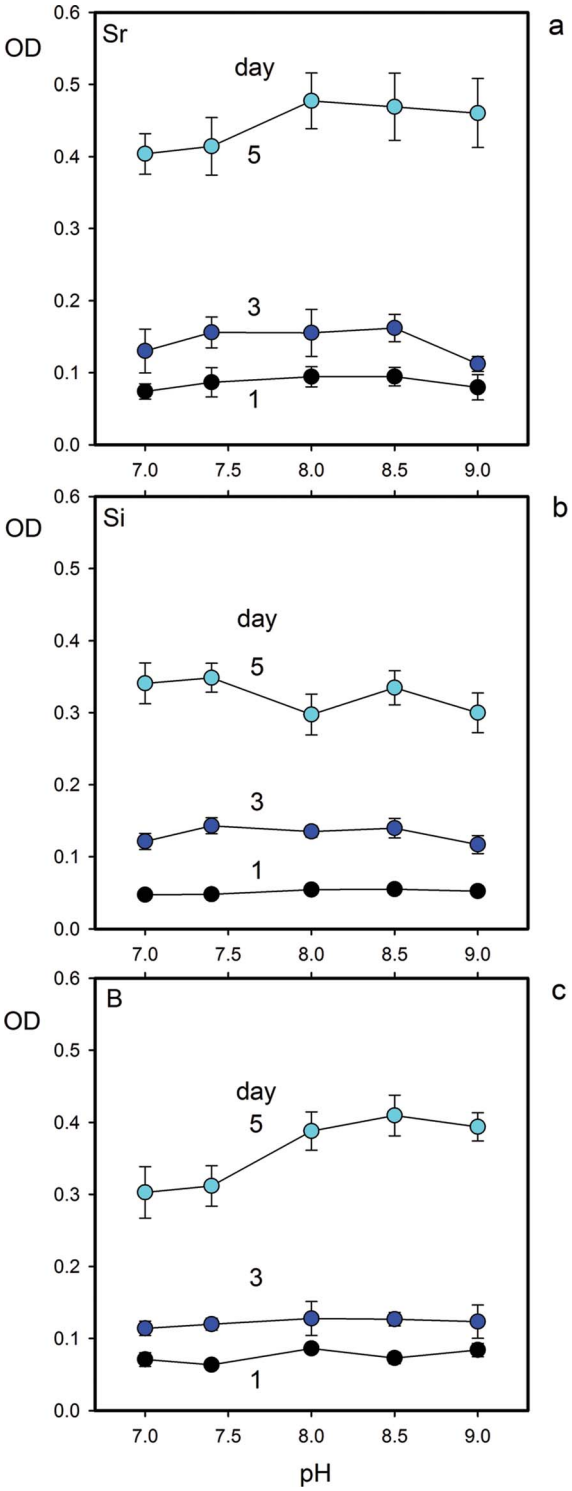

Fig. 3 Effect of pH on MC3T3-E1 osteoblast activity at concentrations of Sr, Si and B giving maximum OD values in Fig. 2: [Si] = 1 mmol L^{-1}; [Sr] = 5 mmol L^{-1}; [B] = 1 mmol L^{-1}.

3. Results

3.1 MC3T3-E1 viability

The pH had a marked effect on the cell viability (Fig. 1). Even on day 5, for pH 5 and 5.5 the OD values were significantly lower than for pH ≥ 6 (both $p = 0.005$, *vs.* pH 6), while the sharp maximum at pH 8 was distinct from the control at pH 7.4 ($p = 0.023$). Strontium and silicon both enhanced proliferation at pH 7.4, with peak values at 5 and 1 mmol L^{-1}, respectively (Fig. 2a,b), although Si was cytotoxic at 5 mmol L^{-1}. Boron had no beneficial effect at any concentration at pH 7.4, indeed,

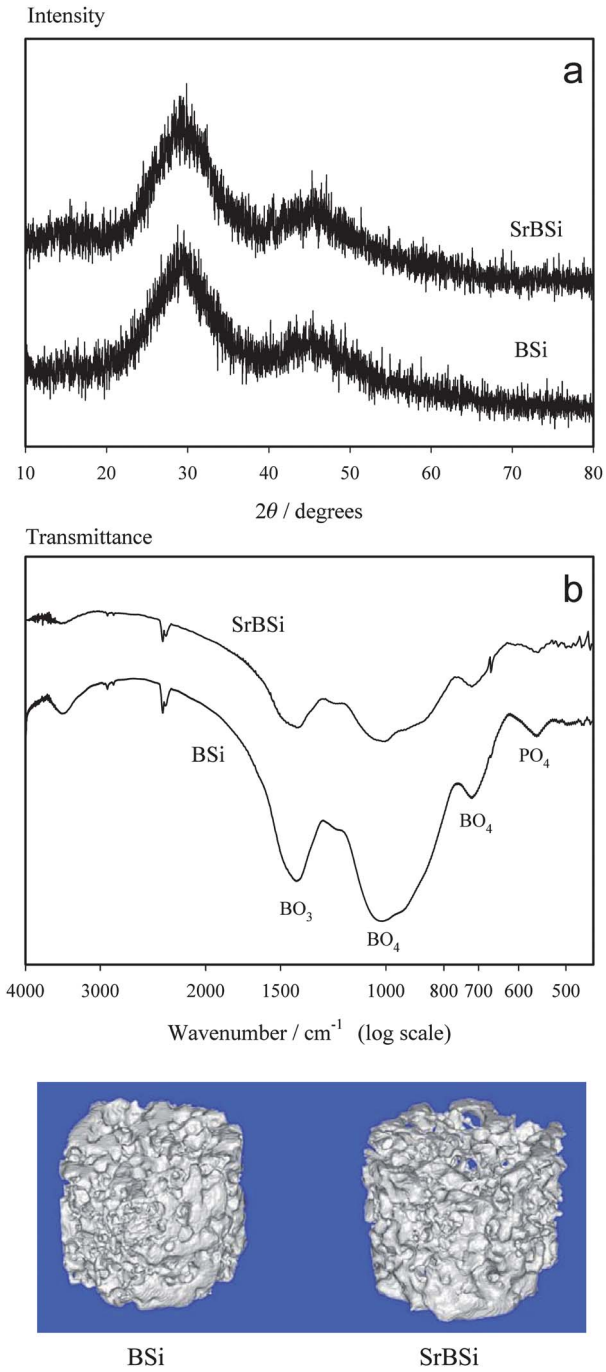

Fig. 4 Characterization of the prepared scaffolds by (a) XRD, (b) FTIR, (c) micro-CT.

cytotoxicity was apparent at day 5 at 2 mmol L^{-1} (Fig. 2c). The effect of pH on the response to the apparent peak concentration of Si (1 mmol L^{-1}) was not significant (Fig. 3a), but was detectable at pH 8.0 for 5 mmol L^{-1} Sr ($p = 0.047$, *vs.* pH 7.4) (Fig. 3b), and at pH 8.5 for 1 mmol L^{-1} B ($p = 0.035$, *vs.* pH 7.4) (Fig. 3c).

3.2 Scaffold characterization

XRD showed that both BSi and SrBSi were amorphous (Fig. 4a). The FTIR spectra (Fig. 4b) were dominated by broad peaks at 600–800 and 800–1200 cm^{-1}, which are the main features of B–O stretching of tetrahedral [BO_4] units, but with a strong absorption band at 1200–1500 cm^{-1}, attributed to B–O stretching in trigonal [BO_3] units, indicating that the main glass network for BSi was [BO_3] and [BO_4]. Weak peaks at 415 and 668 cm^{-1} were

Table 1 Strength and porosity of the present glasses and other scaffold materials

Materials	Compressive strength/MPa	Porosity (%)	Ref.
BSi	4.6 ± 0.8	73.3 ± 2.8	[this paper]
SrBSi	4.5 ± 0.5	73.2 ± 3.5	[this paper]
Sr-Ca_2ZnSiO_7	2.16 ± 0.52	78	22
Ca_2ZnSiO_7	1.99 ± 0.45	77.5	22
$CaSiO_3$	0.32 ± 0.11	81	22
HA	0.03–0.29	69–86	22
45S5 bioglass	0.42–0.60	84–89	22
Spongy bone	0.2–4.0	70–90	22

Table 2 Chemical composition (mol%) of borosilicate scaffold determined by ICP-OES, SrB was prepared by 6 mol% MgO substituted by SrO. *a*: theoretical value; *b*: experimental value with standard deviation (mean ± SD, $n = 5$). The calculated composition is close to that expected

	BSi		SrBSi	
Oxide	*a*	*b*	*a*	*b*
Na_2O	6	6.3 ± 0.6	6	6.8 ± 0.7
K_2O	8	7.1 ± 0.7	8	6.9 ± 0.5
MgO	8	7.9 ± 0.4	2	1.6 ± 0.3
CaO	22	22.2 ± 1.1	22	21.7 ± 1.9
SrO	0	0	6	5.9 ± 0.8
SiO_2	18	17.8 ± 2.3	18	19.4 ± 2.3
B_2O_3	36	36.0 ± 2.6	36	35.9 ± 1.4
P_2O_5	2	1.7 ± 0.3	2	1.8 ± 0.5

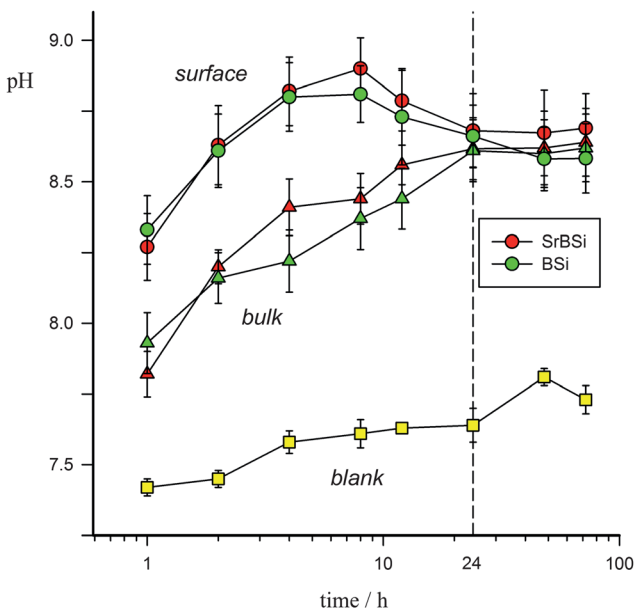

Fig. 5 Surface and bulk pH variation of the medium in contact with the SrBSi and BSi scaffolds.

indicative of Si–O–B linkages, while the peak at 560 cm^{-1} originates from internal modes of the PO_4^{3-} ion. The 3-D structure of the scaffolds is shown in Fig. 4c. The porosity was measured as 73.3 ± 2.8% (BSi) and 73.2 ± 3.5% (SrBSi), and the compressive strength as 4.6 ± 0.8 MPa and 4.5 ± 0.5 MPa respectively, appreciably higher than for other reported scaffold materials (Table 1). The analytical degree of substitution was close to the design value (Table 2), suggesting that the glass network with and without Sr was formed as expected, with no appreciable structural differences due to the incorporation of strontium.

3.3 Degradation behaviour

Upon immersion of the scaffold materials, a difference of pH was apparent between the material surface and the bulk solution, but there was no significant difference between the materials at any time (Fig. 5). The surface pH rose to ~9 in 8 h (SD = ±0.1, $n = 5$), then slightly decreased, apparently stabilizing at ~pH 8.6 (SD = ±0.1, $n = 5$). In contrast, the bulk pH increased steadily and became indistinguishable from the surface value by about 24 h. The rate of dissolution of the material was consistently lower in the case of SrBSi for both B ($F_{1,64} = 5.153$, $P \sim 0.027$) and Si ($F_{1,64} = 11.107$, $P \sim 0.0014$) (2 × AoV, between materials within occurrences) (Fig. 6). The release of the Sr positively affected the viability of the osteoblasts (Fig. 6): at 24 h, both the OD and ALP activity values for the SrBSi extracts were significantly higher than for BSi at pH 8.6; the differences at pH 7.4 were not (Fig. 7).

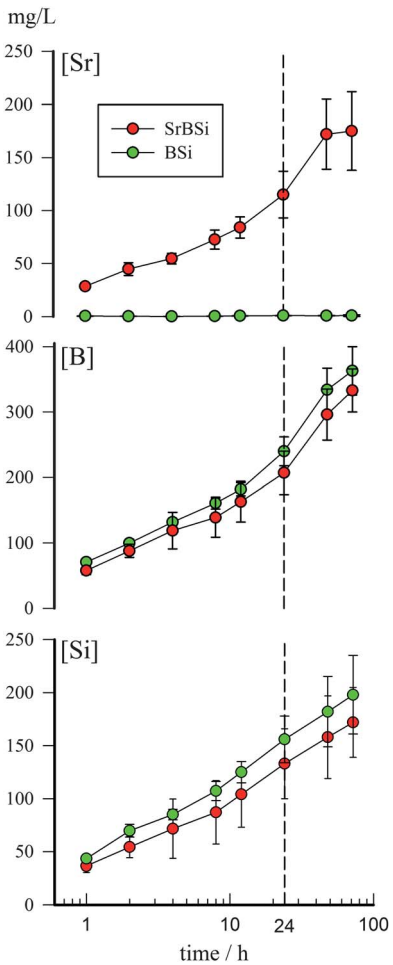

Fig. 6 Concentration of the extracted ions in the medium in contact with the SrBSi and BSi scaffolds.

3.4 Histological images

The new bone formation at the defects was evaluated using Giemsa-Eosin staining in the PMMA-embedded, undecalcified sections. In week 4, new bone could be found adjacent to the BSi scaffold, mainly detected at the interface with the old bone (Fig. 8a), while for SrBSi new bone was formed in the pores of

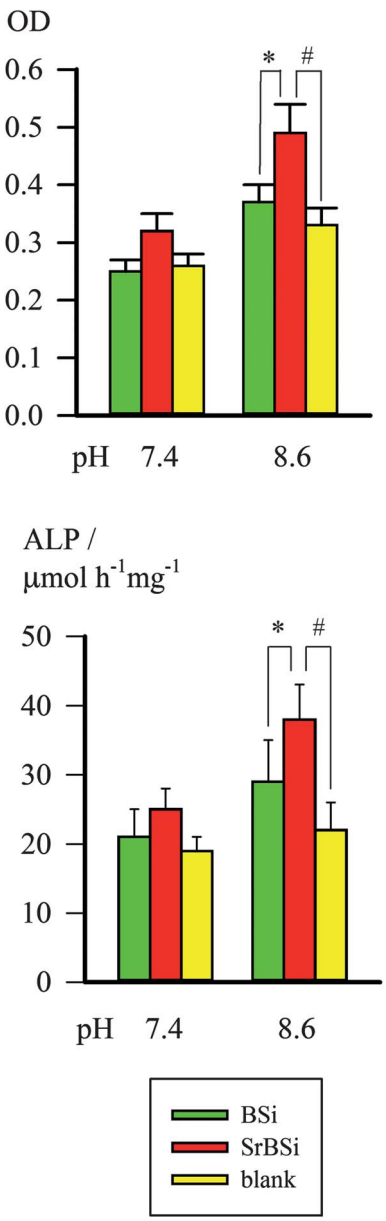

Fig. 7 Proliferation (top) and ALP activity of osteoblasts with respect to pH and scaffold material in contact. Significant comparisons: * $p < 0.05$; # $p < 0.01$.

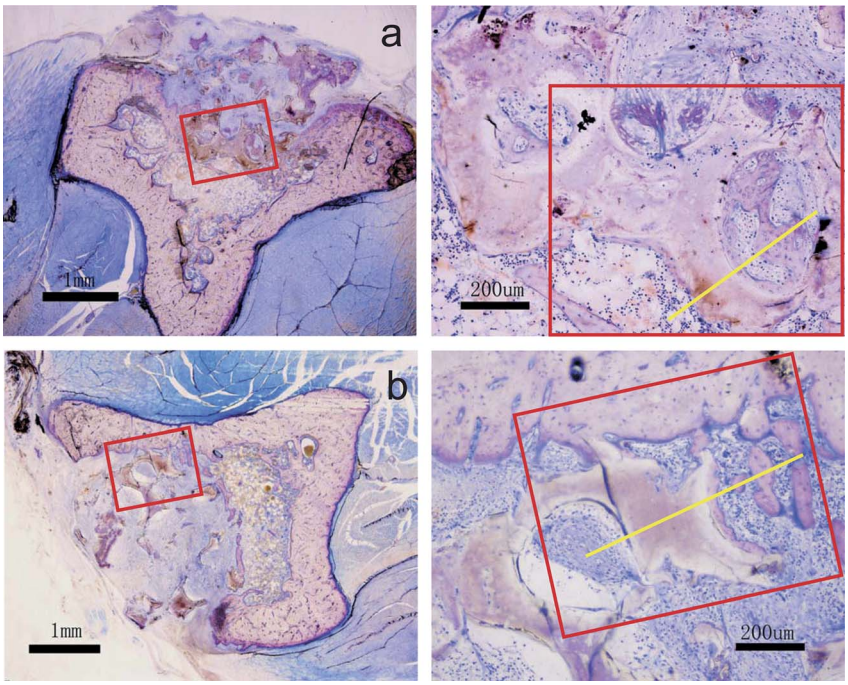

Fig. 8 Giemsa-Eosin stained sections of scaffold-implanted tibiae after 4 weeks. (a) SrBSi and (b) BSi. Left: approximate areas of right-hand image; Right: approximate area and scan line of Fig. 10 images.

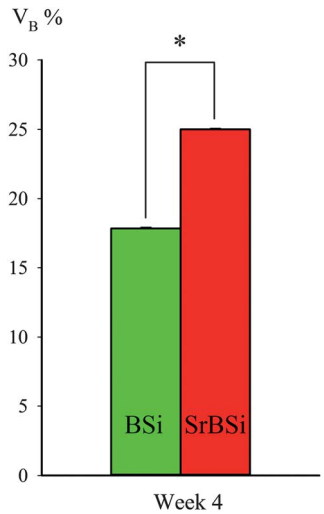

Fig. 9 Comparison of new bone volume fraction, V_B, formed against BSi and SrBSi scaffolds: * $p < 0.05$.

the scaffold (Fig. 8b). The contrast, as measured by V_B, was significant (Fig. 9).

3.5 Chemical analysis

In week 4, significant new bone formation was detected in both scaffolds, as indicated by the analysis showing Ca and P). The new bone layer was found by XRD to contain poorly-crystalline HA, perhaps indicating immaturity (Fig. 10a,b).

4. Discussion

Osteoblasts, the cells responsible for bone formation, have a complex dependence on their immediate environment: not only does the drug dosage matter, but so does the pH. It is now confirmed that their activity is favoured at a pH value greater than that of normal physiological conditions, *i.e.*, pH > 7.4. The results now indicate an optimum value around pH 8 (Fig. 1). In contrast, the activity was dramatically decreased at pH < 6.5. This might suggest that the loss of bone mineral in osteoporotic patients may be associated with chronic acidosis. While a blood pH < ~7.35 is a signal of a potentially serious and dangerous disease state, it seemingly cannot fall much below 7. This, of course, does not rule out the possibility of a low local pH in tissue, especially with osteoclast activity. However, the importance of pH as a controlling factor in the biological process of mineralization appears to have never been properly discussed with the necessary emphasis, although it is known that the local pH must vary during implant degradation.

Here, the principal indicator of the effect of increased pH was in the area of new bone formed. This cannot be attributed simply to driving the precipitation reaction by the increase in [OH^-]:

$$5Ca^{2+} + 3PO_4^{3-} + OH^- \rightarrow Ca_5(PO_4)_3OH$$

because the new material appears to be properly organized tissue and not some random (pathological) calcification (Fig. 8). Quite clearly, under normal physiological conditions, tissue fluid cannot be supersaturated with respect to hydroxyapatite, or any calcium phosphate.[26] Heterogeneous nucleation would result in the immediate and catastrophic precipitation of calcium phosphate (Ca-P) minerals in muscle, blood, skin and brain. Such

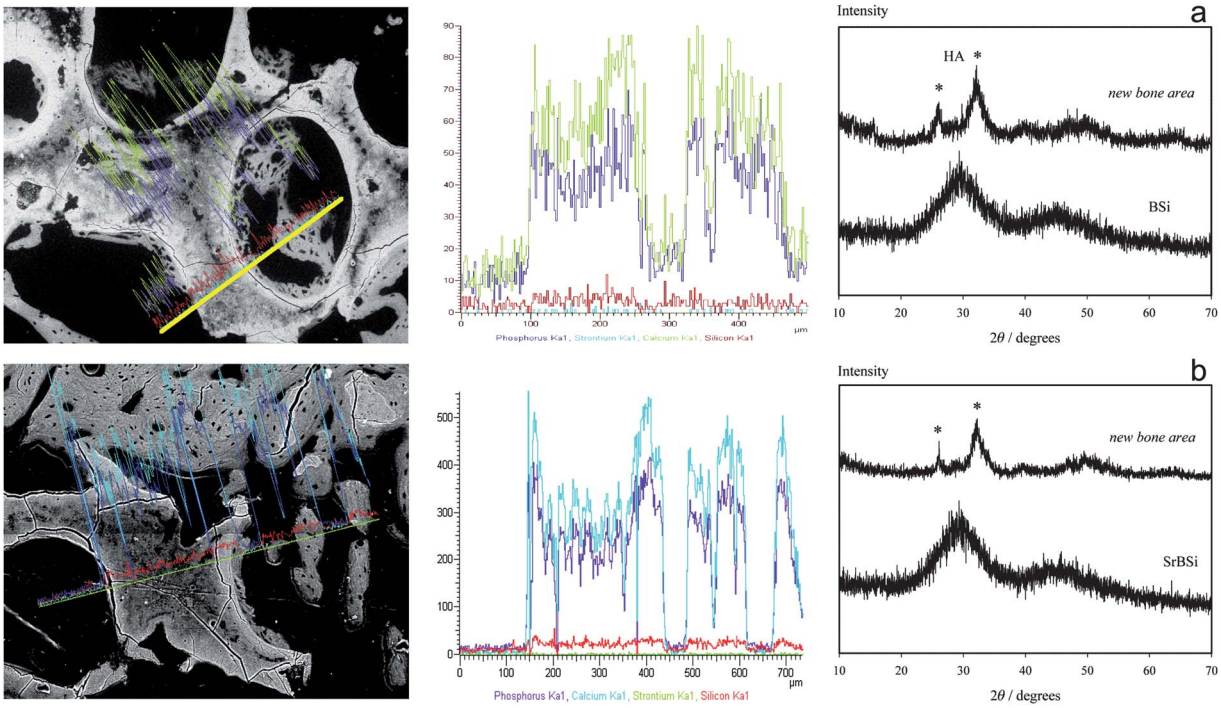

Fig. 10 EDX scans of regions of newly-formed bony structure: (a) SrBSi, (b) BSi. Calcium- and phosphorus-rich regions in the new bone areas identified as poorly-crystalline HA by XRD.

nucleation events would include bruising, foreign body penetration (including deliberate subcutaneous injections, surgical intervention and body piercing), thrombosis, and joint stress as in extreme exercise, to say nothing of the exposure of bone minerals at fractures. Pathology aside, this does not happen. Calcified emboli do not occur. Simply put, we do not spontaneously calcify. However, while a sufficient increase in the pH may tend to drive precipitation, the proliferation and increased activity of osteoblasts is now also anticipated. Both factors therefore facilitate the formation of new bone.

Nevertheless, the measured pH for an extract of any implant material is unlikely to represent that occurring where it matters, *i.e.*, at the material's surface. The local pH can differ significantly from that of the bulk due to implant degradation and diffusion-limited mixing, as indeed is demonstrated here (Fig. 5). However, with time, the values coincided as the degradation rate decreased and diffusion operated, but this was not a tissue-like system. Thus, if an elevated pH is instrumental, the diffusion barrier represented by adjacent tissue, blood clots or deposited extracellular matrix, would also need to be taken into account.

In any case, the optimal pH for bone formation must depend not only on any direct chemical effect but also on its influence on osteoblast activity. Thus, while strontium, a dual anti-resorptive and anabolic drug, has been suggested as a daily oral supplement for osteoporosis treatment, and the dose-dependent effects have been widely reported,[27–29] the role of pH has yet to be mentioned. The findings here that a further increase of osteoblast activity occurs at higher pH values, say ~8–8.5, suggests a new approach to enhance the effect of relevant drug delivery. Boron, although an important trace element for humans (at least), showed no positive effects on the osteoblast activity at any concentration (Fig. 2c), there was nevertheless an apparent increase in the cell activity at pH ~8.5 (Fig. 3c). Thus, bone formation was found in the BSi scaffold after 4 weeks and not only proliferation but the ALP activity was also enhanced (Fig. 7). In addition, a higher bone volume was found with SrBSi, suggesting that the activity of Sr was also enhanced at the higher pH (Fig. 9); again, significantly higher proliferation and ALP activity was found. This is taken to indicate that not only the dosage, but also the pH is key for the stimulation of bone formation.

No pH effect was found for Si (Fig. 3), only for concentration, where the optimal value occurred at 1 mmol L^{-1} (Fig. 2). Thus, while Si released from 45S5 bioglass may indeed stimulate proliferation, this is apparently pH-independent. Even so, the local pH increase that occurs may facilitate the formation of a calcium phosphate layer, and thus the spontaneous bonding to bone.[21,30] Thus, upon implant degradation, account has to be taken of not only the released ions, but also their effect on the local environment, in particular, the pH, neglect of which may result in the misunderstanding of a crucial step in bone formation. Nevertheless, the variation occurring in this respect between implant materials has to be recognized in terms of composition, constitution, morphology and structure. There is work yet to be done.

Conclusion

Overall, it would seem that because pH plays an important role in modulating osteoblast activity, and also affects positively the effects of strontium and boron, attention needs to be given to the interaction of all such factors. Obviously, in the face of such synergism, simplistic single-factor exploration is insufficient, and a more complete exploration of the evidently multifactorial system is required to identify the global optimum, rather than

merely several local optima. While such optima may be suggestive, they cannot stand alone.

Acknowledgements

This work was funded by grants from NSFC/RGC (Grant No.: N_HKU 739/10), HKU Seed Funding Programme for Basic Research, No: 201110159010, and the Natural Science Foundation of China (No.: 51072133). The authors are grateful for much technical support and guidance from the Electron Microscopy Unit of The University of Hong Kong.

References

1 J. Chau, W. Leong and B. Li, *Histol. Histopathol.*, 2009, **24**, 1593.
2 U. Iwaniec, T. Wronski, J. Liu, M. Rivera, R. Arzaga, G. Hansen and R. Brommage, *J. Bone Miner. Res.*, 2007, **22**, 394.
3 X. Y. Tian, W. S. S. Jee, M. Setterberg, M. Chen, X. Li, W. S. Simonet, C. Paszty and H. Z. Ke, *Bone*, 2008, **43**, S29.
4 Y. Seino, S. Ishizuka, M. Shima and H. Tanaka, *Osteoporosis Int.*, 1993, **3**, 196.
5 M. Kashii, J. Hashimoto, T. Nakano, Y. Umakoshi and H. Yoshikawa, *J. Bone Miner. Metab.*, 2008, **26**, 24.
6 T. Arnett, *J. Nutr.*, 2008, **138**, 415.
7 S. Meghji, M. Morrison, B. Henderson and T. Arnett, *Am. J. Physiol. Endocrinol. Metab.*, 2001, **280**, E112.
8 D. Bushinsky, *Am. J. Physiol.*, 1996, **271**, F216.
9 D. Bushinsky, *Eur. J. Nutr.*, 2001, **40**, 238.
10 J. Kaunitz and D. Yamaguchi, *J. Cell. Biochem.*, 2008, **105**, 655.
11 M. Harada, N. Udagawa, K. Fukasawa, B. Hiraoka and M. Mogi, *J. Dent. Res.*, 1986, **65**, 125.
12 Y. Shen, W. Liu, K. Lin, H. Pan, B. Darvell, S. Peng, C. Wen, L. Deng, W. Lu and J. Chang, *Langmuir*, 2011, **27**, 2701.
13 X. Zhang, W. Jia, Y. Gu, W. Xiao, X. Liu, D. Wang, C. Zhang, W. Huang, M. Rahaman, D. Day and N. Zhou, *Biomaterials*, 2010, **31**, 5865.
14 A. Yao, D. Wang, W. Huang, Q. Fu, M. Rahaman and D. Day, *J. Am. Ceram. Soc.*, 2007, **90**, 303.
15 F. Nielsen, *Nutrition*, 2000, **16**, 512.
16 D. Garrett, *Borates: handbook of deposits, processing, properties, and use*, Academic Press, San Diego, CA, 1998.
17 F. Nielsen, *Biol. Trace Elem. Res.*, 1990, **9**, 61.
18 P. Xu, W. Hu, X. Guo, Y. Zhang, Y. Li, J. Yao and Q. Cai, *J. South. Med. Univ.*, 2006, **26**, 1785.
19 F. Nielsen, C. Hunt, L. Mullen and J. Hunt, *FASEB J.*, 1987, **1**, 394.
20 H. Pan, X. Zhao, X. Zhang, K. Zhang, L. Li, Z. Li, W. Lam, W. Lu, D. Wang, W. Huang, K. Lin and J. Chang, *J. R. Soc. Interface*, 2009, **7**, 1025.
21 L. Hench, *J. Mater. Sci.: Mater. Med.*, 2006, **17**, 967.
22 H. Zreiqat, Y. Ramaswamy, C. Wu, A. Paschalidis, Z. Lu, B. James, O. Birke, M. McDonald, D. Little and C. Dunstan, *Biomaterials*, 2010, **31**, 3175.
23 W. Huang, D. Day, K. Kittiratanapiboon and M. Rahaman, *J. Mater. Sci.: Mater. Med.*, 2006, **17**, 583.
24 X. Liu, W. Huang, H. Fu, A. Yao, D. Wang, H. Pan and W. Lu, *J. Mater. Sci.: Mater. Med.*, 2009, **20**, 365.
25 A. Parfitt, M. Drezner, F. Glorieux, J. Kanis, H. Malluche, P. Meunier, S. Ott and R. Recker, *J. Bone Miner. Res.*, 1987, **2**, 595.
26 H. B. Pan, X. L. Zhao, B. W. Darvell and W. W. Lu, *Acta Biomater.*, 2010, **6**, 4181.
27 P. Marie, *Osteoporosis Int.*, 2008, **19**, 1813.
28 J. Liu, K. A. Wai-Chee, C. Pheng, H. Zhu, Z. Zhang, Y. Wu, L. Xu, X. Meng, M. Huang, L. Chung, N. Hussain, S. Sufian and J. Chen, *Bone*, 2009, **45**, 460.
29 L. Dominguez, R. Scalisi and M. Barbagallo, *Acta Biomed.*, 2010, **81**, 55.
30 M. Cerruti, D. Greenspan and K. Powers, *Biomaterials*, 2005, **26**, 1665.

